Cascaded and Sum of Cascaded Over $\alpha-\mathcal{F}$ Fading Channels With Pointing Error Impairment

PEDRO H. D. ALMEIDA [1] **(Graduate Student Member, IEEE),**
HUGERLES S. SILVA [1,2] **(Senior Member, IEEE), UGO S. DIAS** [1] **(Senior Member, IEEE), RAUSLEY A. A. DE SOUZA** [3,4] **(Senior Member, IEEE), IGUATEMI E. FONSECA** [5] **, AND YONGHUI LI** [1] **(Fellow, IEEE)**

[1]Department of Electrical Engineering, University of Brasília, Brasília 70910-900, Brazil
[2]Instituto de Telecomunicações and Departamento de Eletrónica, Telecomunicações e Informática, Universidade de Aveiro, Campus Universitário de Santiago, 3810-193 Aveiro, Portugal
[3]National Institute of Telecommunications (Inatel), Santa Rita do Sapucaí 37540-000, Brazil
[4]School of Electrical and Information Engineering, University of Sydney, Sydney, NSW 2006, Australia
[5]Informatics Center, Federal University of Paraíba, João Pessoa 58051-900, Brazil

CORRESPONDING AUTHOR: HUGERLES S. SILVA (e-mail: hugerles.silva@av.it.pt).

ABSTRACT In this article, exact expressions are presented for the probability density function, cumulative distribution function, moment generating function, and higher-order moments of the instantaneous signal-to-noise ratio, considering the product and the sum of the products of N $\alpha-\mathcal{F}$ variates with pointing errors. New expressions for the outage probability (OP), bit error probability (BEP), ergodic channel capacity, and the area under the receiver operating characteristics (AUC) are deduced, as well as the asymptotic ones. The obtained expressions are used to assess the influence of various channels and system parameters on the system performance. We analyze a scenario considering dual-hop terahertz links and another regarding reconfigurable intelligent surfaces (RIS)-assisted systems. All expressions derived in this work are new, and Monte Carlo simulations corroborate the analytical curves shown.

INDEX TERMS $\alpha-\mathcal{F}$ fading, AUC, BEP, capacity, OP, pointing errors, RIS, terahertz links.

I. INTRODUCTION

Cascaded and sum of cascaded fading channels have been considered in several practical applications, such as multihop and reconfigurable intelligent surfaces (RISs)-based communication systems, and have attracted the interest of researchers [1], [2], [3], [4], [5], [6]. Over the years, the aforementioned channels have been studied considering independent and identically or independent and not necessarily identically distributed variates, under generalist [1], [3], [7] or simple fading models [2], [8], [9].

In the literature, many works have also addressed the misalignment between the transmitting and receiving antennas, a phenomenon well-known as pointing error [10], [11]. The phenomenon mentioned affects the received signal strength and thus deteriorates the link performance and availability, which may result in a system outage. This effect is considered in different contexts, such as RIS [12], [13], [14], [15], [16], [17], [18], single-, dual- and multi-hop [11], [19], [20], multiple-input multiple-output (MIMO) [21], and non-orthogonal multiple access terahertz (THz) [22] transmission

systems, for example. It occurs because high-directional antenna arrays are used to compensate the high atmospheric attenuation in the THz bands.

In this work, the cascaded and the sum of cascaded α-$\mathcal{F}$ fading distribution with pointing errors is introduced and mathematically characterized. In our study, the THz channel is jointly composed of the deterministic path loss, the stochastic fading due to the multipath, shadowing, nonlinearity of the medium, and the antenna pointing errors. In order to analyze these effects and design parameters in the technical THz literature, exact and new expressions for important statistics and metrics are presented. An asymptotic analysis is also provided. Furthermore, a scenario considering THz links is analyzed.

In our paper, the α-$\mathcal{F}$ distribution [23] is adopted to model the fading channel since its statistics are simple and written in terms of physical parameters. The α-$\mathcal{F}$ is a fading model that jointly considers the short-term fading (α-μ) and the long-term fading ($\mathcal{F}$ distribution) of a wireless fading channel. In another words, the α-$\mathcal{F}$ is the α-μ shadowed distribution. The model mentioned is supported by experimental results [23], and it is adopted in many works under different real-world scenarios [24], [25], [26], [27]. Note that the α-$\mathcal{F}$ distribution includes other well-known distributions as special cases, such as the α-μ ($m \rightarrow \infty$) and the Fisher-Snedecor $\mathcal{F}$ ($\alpha = 2$) distributions–and their inclusive ones. Furthermore, the α-$\mathcal{F}$ composite fading model considers small and large-scale fading, as well as the non-linearity of the medium [23]. This indicates the promising potential of employing the α-$\mathcal{F}$ distribution to characterize THz channels.

Concerning the pointing error distribution, the one presented in [10] is considered in our study, that is a realistic model and has been successfully adopted in many important papers dealing with THz systems [10], [11], [19], [21], [22], requiring only the use of circular lenses at the transmitter and receiver sides. Furthermore, the statistics of the mentioned distribution are exact and simple. We adopt the aforementioned pointing error model to quantify the impact of the beam misalignment in the system. In the literature, new pointing error models for millimeter wave and THz high-directional antennas are presented [28], [29].

To the best of our knowledge, this is the first work in which the cascaded and the sum of cascaded α-$\mathcal{F}$ fading distribution with pointing errors is studied. All expressions derived by us are new and generalist, written in terms of the single or multivariate Fox H-function [30]. The aforementioned expressions can be applied in different scenarios, including THz, RIS-assisted communications, multi-hop amplify and forward non-regenerative relaying systems, MIMO keyhole, or single-hop multiple-input single-output (MISO) systems, for example.

The main contributions of this article are: (i) New closed-form expressions for the probability density function (PDF), cumulative distribution function (CDF), and moment generating function (MGF) of the instantaneous signal-to-noise ratio (SNR), considering the cascaded and the sum of cascaded α-$\mathcal{F}$ fading with pointing errors; (ii) New expressions for outage probability (OP), bit error probability (BEP), ergodic channel capacity, and area under the receiver operating characteristics (AUC), under cascaded α-$\mathcal{F}$ fading with pointing errors; (iii) A new OP expression for the sum of cascaded α-$\mathcal{F}$ fading with pointing errors which is used to assess the performance of RIS-assisted systems; and (iv) Asymptotic expressions are also deduced to provide insights into the effect of the channel and pointing error parameters on the system performance at a high SNR regime.

The remainder of the paper is organized as follows. In Sections II and III, respectively, statistics and metrics are derived for the cascaded and sum of cascaded of α-$\mathcal{F}$ composite fading distribution with pointing errors. Section IV shows the numerical results and discussions. Section V brings the conclusions.

II. CASCADED α-$\mathcal{F}$ FADING WITH POINTING ERRORS CHANNELS

A. CASCADED SYSTEM MODEL

The cascaded fading coefficient can be written as $H = H_1 H_2 \cdots H_N$, whose $H_j = h_{l_j} H_{f_j} H_{p_j}$, $j = 1, 2, \ldots, N$. The H_j PDF is given by

$$
f_{H_j}(h_j)
$$

$$
= \frac{\mathrm{H}_{2,2}^{2,1}\left[\Psi_j \left(\frac{h_j}{\hat{r}_j h_{l_j} A_{0j}} \right)^{\alpha_j} \middle| \begin{array}{l} (1-m_j, 1), (z_j^2/\alpha_j + 1, 1) \\ (\mu_j, 1), (z_j^2/\alpha_j, 1) \end{array} \right]}{h_j \Gamma(\mu_j) \Gamma(m_j)/z_j^2},
$$

(1)

where H_j is the j-th envelope fading channel characterized by the α-$\mathcal{F}$ composite distribution with pointing errors for each THz link [31, Eq. (4)], $\Psi_j = \mu_j/(m_j - 1)$, $\hat{r}_j = \sqrt[\alpha_j]{\mathbb{E}[H_{f_j}^{\alpha_j}]}$ is the α-root mean value, α_j characterizes the non-linearity of the propagation medium, μ_j represents the number of multipath clusters, m_j is the shadowing parameter, $\Gamma(\cdot)$ is the Gamma function, $\mathrm{H}[\cdot]$ denotes the Fox H-function, A_{0j} is the fraction of the collected power, and z_j is the ratio between the equivalent beam radius at the receiver and the pointing error displacement standard deviation. For $z_j \rightarrow \infty$, it should be mentioned that the case of the non-pointing error is assumed.

It is assumed a THz link model with highly-directional transmit and receive antennas to ensure reliable energy transmission. In this model, H_{f_j} denotes the composite fading channel, H_{p_j} represents the misalignment component, and $h_{l_j} = h_{fl_j} h_{al_j}$ is the deterministic path loss that is constant for a given weather condition and link distance. The parameter h_{fl_j} models the propagation gain and is given by

$$
h_{fl_j} = \frac{c G_{t_j} G_{r_j}}{4\pi f d_j},
$$

(2)

in which G_{t_j} and G_{r_j} are, respectively, the gains of the transmit- and receive-antenna, c is the speed of light, f is the operating frequency, and d_j is the distance of the j-th hop such that $\sum_{j=1}^{N} d_j$ is the total distance of the link. In addition, h_{al_j}

characterizes the molecular absorption gain and is given by

$$h_{\text{al}_j} = \exp\left(-\frac{1}{2}\kappa_j(f)d_j\right), \tag{3}$$

in which $\kappa_j(f)$ denotes the frequency-dependent absorption coefficient. More details about h_{1_j} can be found in [11]. Thus, the received signal considering a wireless multi-hop amplify-and-forward relaying link can be written as

$$Y = \underbrace{H_1 H_2 H_3 \cdots H_N}_{H} X + W, \tag{4}$$

where X is the transmitted signal and W is the additive white Gaussian noise with zero mean and variance σ_W^2.

B. FIRST ORDER STATISTICS

Lemma 2.1: Let $\alpha_j, \mu_j, \bar{\gamma}_j, z_j, A_{0_j}, h_{1_j}, s, \gamma \in \mathbb{R}^+$, and $m_j > 1$, with $j = 1, 2, \ldots, N$. The PDF, the CDF, and the MGF of the instantaneous SNR Γ, under cascaded α-$\mathcal{F}$ composite fading with pointing errors, are given, respectively, by

$$f_\Gamma(\gamma) = \frac{H_{2N,2N}^{2N,N}\left[\Xi\sqrt{\gamma} \;\middle|\; \begin{matrix} \mathcal{A}_1, \ldots, \mathcal{A}_N, \mathcal{B}_1, \ldots, \mathcal{B}_N \\ \mathcal{C}_1, \ldots, \mathcal{C}_N, \mathcal{D}_1, \ldots, \mathcal{D}_N \end{matrix}\right]}{2\gamma \prod_{j=1}^N \alpha_j \Gamma(\mu_j)\Gamma(m_j)/z_j^2}, \tag{5}$$

$$F_\Gamma(\gamma)$$
$$= \frac{H_{2N+1,2N+1}^{2N,N+1}\left[\Xi\sqrt{\gamma} \;\middle|\; \begin{matrix} (1,1), \mathcal{A}_1, \ldots, \mathcal{A}_N, \mathcal{B}_1, \ldots, \mathcal{B}_N \\ \mathcal{C}_1, \ldots, \mathcal{C}_N, \mathcal{D}_1, \ldots, \mathcal{D}_N, (0,1) \end{matrix}\right]}{\prod_{j=1}^N \alpha_j \Gamma(\mu_j)\Gamma(m_j)/z_j^2}$$
$$\tag{6}$$

and

$$M_\Gamma(s)$$
$$= \frac{H_{2N+1,2N}^{2N,N+1}\left[\frac{\Xi}{\sqrt{s}} \;\middle|\; \begin{matrix} (1,\frac{1}{2}), \mathcal{A}_1, \ldots, \mathcal{A}_N, \mathcal{B}_1, \ldots, \mathcal{B}_N \\ \mathcal{C}_1, \ldots, \mathcal{C}_N, \mathcal{D}_1, \ldots, \mathcal{D}_N \end{matrix}\right]}{2\prod_{j=1}^N \alpha_j \Gamma(\mu_j)\Gamma(m_j)/z_j^2}, \tag{7}$$

where $\mathcal{A}_j = (1 - m_j, 1/\alpha_j)$, $\mathcal{B}_j = (z_j^2/\alpha_j + 1, 1/\alpha_j)$, $\mathcal{C}_j = (\mu_j, 1/\alpha_j)$, $\mathcal{D}_j = (z_j^2/\alpha_j, 1/\alpha_j)$, and $\Xi = \prod_{j=1}^N \Psi_j^{\frac{1}{\alpha_j}}$

$z_j/\sqrt{\bar{\gamma}_j(z_j^2 + 2)}$, in which $\bar{\gamma}_j$ is the average SNR and N is the number of channels.

Proof: See Appendix A. ∎

C. PERFORMANCE METRICS
1) BIT ERROR PROBABILITY
The average BEP, P_b, can be evaluated as

$$P_b = \frac{1}{\pi}\int_0^{\frac{\pi}{2}} M_\Gamma\left(\frac{\rho}{\sin^2\phi}\right)d\phi, \tag{8}$$

in which ρ depends on the modulation type assumed.

Substituting (7) into (8), making the variable change $x = \sin^2(\phi)$, using [32, id 06.18.07.0001.01], [32, id 06.18.02.0001.01], and performing some simplifications, it follows that (9), shown at the bottom of this page, is obtained.

2) OUTAGE PROBABILITY
The OP, P_{out}, is defined as the point at which the SNR of the signal at the output of the receiver falls below the threshold γ_{th}, i.e. $P_{\text{out}} \triangleq \text{Prob}[\Gamma \leq \gamma_{\text{th}}] = F_\Gamma(\gamma_{\text{th}})$. Then, (10), shown at the bottom of this page, is deduced.

3) ERGODIC CHANNEL CAPACITY
The ergodic channel capacity, in bit/s, is calculated as

$$C_{\text{erg}} = \frac{1}{\ln(2)}\int_0^\infty f_\Gamma(\gamma)\ln(1+\gamma)d\gamma. \tag{13}$$

Replacing (5) into (13) and using [32, 01.04.26.0003.01] and [33, Eq. (2.8.4)], the channel capacity can be written as (11) shown at the bottom of this page.

4) AVERAGE AUC
The average AUC, $\bar{A}$, is given by [34, Eq. (36)]

$$\bar{A} = \int_0^\infty A(\gamma)f_\Gamma(\gamma)d\gamma, \tag{14}$$

in which $A(\gamma)$ denotes the instantaneous AUC [34, Eq. (35)] given by

$$A(\gamma) = 1 - \sum_{k=0}^{u-1}\sum_{l=0}^k \binom{k+u-1}{k-l}\frac{\gamma^l \exp(-\gamma/2)}{2^{k+l+u}l!}, \tag{15}$$

$$P_b = \frac{H_{2N+2,2N+1}^{2N,N+2}\left[\frac{\Xi}{\sqrt{\rho}} \;\middle|\; \begin{matrix} (1,\frac{1}{2}), (\frac{1}{2},\frac{1}{2}), \mathcal{A}_1, \ldots, \mathcal{A}_N, \mathcal{B}_1, \ldots, \mathcal{B}_N \\ \mathcal{C}_1, \ldots, \mathcal{C}_N, \mathcal{D}_1, \ldots, \mathcal{D}_N, (0,\frac{1}{2}) \end{matrix}\right]}{4\sqrt{\pi}\prod_{j=1}^N \alpha_j \Gamma(\mu_j)\Gamma(m_j)/z_j^2} \tag{9}$$

$$P_{\text{out}} = \frac{H_{2N+1,2N+1}^{2N,N+1}\left[\Xi\sqrt{\gamma_{\text{th}}} \;\middle|\; \begin{matrix} (1,1), \mathcal{A}_1, \ldots, \mathcal{A}_N, \mathcal{B}_1, \ldots, \mathcal{B}_N \\ \mathcal{C}_1, \ldots, \mathcal{C}_N, \mathcal{D}_1, \ldots, \mathcal{D}_N, (0,1) \end{matrix}\right]}{\prod_{j=1}^N \alpha_j \Gamma(\mu_j)\Gamma(m_j)/z_j^2} \tag{10}$$

$$C_{\text{erg}} = \frac{H_{2N+2,2N+2}^{2N+2,N+1}\left[\Xi \;\middle|\; \begin{matrix} (0,\frac{1}{2}), \mathcal{A}_1, \ldots, \mathcal{A}_N, \mathcal{B}_1, \ldots, \mathcal{B}_N, (1,\frac{1}{2}) \\ \mathcal{C}_1, \ldots, \mathcal{C}_N, \mathcal{D}_1, \ldots, \mathcal{D}_N, (0,\frac{1}{2}), (0,\frac{1}{2}) \end{matrix}\right]}{2\ln(2)\prod_{j=1}^N \alpha_j \Gamma(\mu_j)\Gamma(m_j)/z_j^2} \tag{11}$$

where u denotes the time-bandwidth product under the energy detection technique and $\binom{a}{b}$ is the binomial coefficient. Replacing (5) and (15) in (14), using the integral representation of the H-function, [35, Eq. (3.381.4)] and [30, Eq. (1.2)] in sequence, one obtains (12) shown at the bottom of the page.

D. ASYMPTOTIC ANALYSIS

1) BIT ERROR PROBABILITY AND OUTAGE PROBABILITY

Considering the approach presented in [36], it follows that the asymptotic BEP and OP can be written as

$$P_{\rm b}^{\infty} = \frac{1}{B_\beta} \left[\prod_{j=1}^{N} \frac{z_j^2}{\alpha_j \Gamma(\mu_j)\Gamma(m_j)} \right] \frac{\phi \Gamma\left(\frac{U}{2}\right) \Gamma\left(\frac{U+1}{2}\right)\left(\frac{\Xi}{\sqrt{\rho}}\right)^U}{4\sqrt{\pi}\,\Gamma\left(\frac{U}{2}+1\right)} \tag{16}$$

and

$$P_{\rm out}^{\infty} = \frac{1}{B_\beta} \left[\prod_{j=1}^{N} \frac{z_j^2}{\alpha_j \Gamma(\mu_j)\Gamma(m_j)} \right] \frac{\phi \Gamma(U)\left(\gamma_{\rm th}^{\frac{1}{2}}\Xi\right)^U}{\Gamma(1+U)}, \tag{17}$$

respectively, where $U = \min\{\mu_1\alpha_1, \ldots, \mu_N\alpha_N, z_1^2, \ldots, z_N^2\}$, $\beta = \arg\min U$, and ϕ is given by (18) shown at the bottom of this page. It should be mentioned that B_β is the residual term in the Fox H-function considered by removing the respective Gamma function from the condition $\mu_j \neq \frac{U}{\alpha_j}$ or $z_j^2 \neq U$ in (18).

From (16) and (17), the diversity order of the considered system can be found as

$$G_{\rm d} = \min(\alpha_1\mu_1/2, \ldots, \alpha_N\mu_N/2, z_1^2/2, \ldots, z_N^2/2). \tag{19}$$

That is, the diversity order depends on the fading and pointing error parameters.

2) ERGODIC CHANNEL CAPACITY

The asymptotic ergodic capacity at high SNR values is given by [37]

$$C_{\rm erg}^{\infty} = \log_2(\bar{\gamma}) + \log_2(e) \frac{\partial}{\partial n} \left.\frac{\mathbb{E}[\gamma^n]}{\bar{\gamma}^n}\right|_{n=0}, \tag{20}$$

in which $\partial/\partial n$ is the first derivative operator and

$$\mathbb{E}[\gamma^n] = \frac{\prod_{j=1}^{N} z_j^2 \Gamma\left(\mu_j + \frac{2n}{\alpha_j}\right) \Gamma\left(\frac{z_j^2 + 2n}{\alpha_j}\right) \Gamma\left(m_j - \frac{2n}{\alpha_j}\right)}{\Xi^{2n} \prod_{j=1}^{N} \alpha_j \Gamma(\mu_j)\Gamma(m_j)\Gamma\left(\frac{z_j^2}{\alpha_j} + 1 + \frac{2n}{\alpha_j}\right)}. \tag{21}$$

Replacing (21) into (20) and proceeding with simplifications,

$$C_{\rm erg}^{\infty} = \log_2\left(\frac{1}{\Xi^2}\right) + \log_2(e)\left[\sum_{j=1}^{N} \frac{2}{\alpha_j}\left(\psi(\mu_j) + \psi\left(\frac{z_j^2}{\alpha_j}\right) \right.\right.$$
$$\left.\left. -\psi(m_j) - \psi\left(\frac{z_j^2}{\alpha_j} + 1\right) \right) \right], \tag{22}$$

with $\psi(x) = \Gamma'(x)/\Gamma(x)$ denoting the digamma function [35, Eq. (8.36)].

3) AUC

The asymptotic AUC is given by

$$\bar{A}^{\infty} = 1 - \sum_{k=0}^{u-1}\sum_{l=0}^{k} \binom{k+u-1}{k-l} \frac{\phi\Gamma\left(l + \frac{U}{2}\right)}{2^{k+u+1}l!B_\beta}$$
$$\times \frac{(\sqrt{2}\Xi)^U}{\prod_{j=1}^{N}\alpha_j\Gamma(\mu_j)\Gamma(m_j)/z_j^2}, \tag{23}$$

that is derived from (12) using the approach presented in [36].

III. SUM OF CASCADED α-$\mathcal{F}$ FADING WITH POINTING ERROR CHANNELS

A. SYSTEM MODEL

Let S be the sum of products of N α-$\mathcal{F}$ RVs with pointing errors, i.e.,

$$S = \sum_{i=1}^{L} H_{i1}H_{i2}\cdots H_{iN} = \sum_{i=1}^{L}\prod_{j=1}^{N} H_{ij}, \ \ L \geq 1, \ N \geq 1. \tag{24}$$

The received signal, under the aforementioned model, can be written as

$$Y = \underbrace{\sum_{i=1}^{L} H_{i1}H_{i2}\cdots H_{iN}}_{S} X + W. \tag{25}$$

$$\bar{A} = 1 - \sum_{k=0}^{u-1}\sum_{l=0}^{k} \binom{k+u-1}{k-l} \frac{1}{2^{k+u+1}l!} \frac{{\rm H}^{2\,N,N+1}_{2N+1,2\,N}\left[\sqrt{2}\Xi \left| \begin{array}{c}(1-l,1/2), \mathcal{A}_1, \ldots, \mathcal{A}_N, \mathcal{B}_1, \ldots, \mathcal{B}_N \\ \mathcal{C}_1, \ldots, \mathcal{C}_N, \mathcal{D}_1, \ldots, \mathcal{D}_N \end{array}\right.\right]}{\prod_{j=1}^{N}\alpha_j\Gamma(\mu_j)\Gamma(m_j)/z_j^2} \tag{12}$$

$$\phi = \frac{\prod_{\substack{j=1 \\ \mu_j \neq \frac{U}{\alpha_j}}}^{N} \Gamma\left(\mu_j - \frac{U}{\alpha_j}\right) \prod_{\substack{j=1 \\ z_j^2 \neq U}}^{N} \Gamma\left(\frac{z_j^2 - U}{\alpha_j}\right) \prod_{j=1}^{N} \Gamma\left(m_j + \frac{U}{\alpha_j}\right)}{\prod_{j=1}^{N} \Gamma\left(\frac{z_j^2}{\alpha_j} + 1 - \frac{U}{\alpha_j}\right)} \tag{18}$$

B. FIRST ORDER STATISTICS

Lemma 3.1: Consider $\alpha_{ij}, \mu_{ij}, \bar{\gamma}_{ij}, z_{ij}, A_{0_{ij}}, h_{l_{ij}}, s, \gamma \in \mathbb{R}^{+}$, and $m_{ij} > 1$, with $j = 1, 2, \ldots, N$ and $i = 1, 2, \ldots, L$. The PDF, the CDF, and the MGF of the instantaneous SNR Γ, considering the sum of independent and non-identically distributed cascaded α-$\mathcal{F}$ RVs with pointing errors, are given by (26), (27) and (28), all shown at the bottom of this page, respectively, where H$[\cdot | \cdot | \cdot]$ is the multivariate Fox H-function [30].

Proof: See Appendix B. ∎

C. PERFORMANCE METRICS

1) OUTAGE PROBABILITY
The OP is given by (29) shown at the bottom of this page.

2) ASYMPTOTIC OUTAGE PROBABILITY
Considering the approach presented in [36], it follows that the asymptotic OP can be written as

$$P_{\text{out}}^{\infty} = \frac{1}{2 \prod_{i=1}^{L} B_{\beta_i}} \left[\prod_{i=1}^{L} \prod_{j=1}^{N} \frac{z_{ij}^2}{\alpha_{ij} \Gamma(\mu_{ij}) \Gamma(m_{ij})} \right]$$

$$\times \Psi(U_1, \ldots, U_L) \left[\prod_{i=1}^{L} \phi \left(\Xi_i \gamma_{\text{th}}^{1/2} \right)^{U_i} \Gamma(U_i) \right], \quad (30)$$

with $\quad U_i = \min\{\mu_{i1}\alpha_{i1}, \ldots, \mu_{iN_i}\alpha_{iN_i}, z_{i1}^2, \ldots, z_{iN}^2\}, \quad \beta_i = $ arg min U_i,

$$\Psi(U_1, \ldots, U_L) = \frac{\Gamma\left(\sum_{i=1}^{L} \frac{U_i}{2}\right)}{\Gamma\left(\sum_{i=1}^{L} U_i\right) \Gamma\left(1 + \sum_{i=1}^{L} \frac{U_i}{2}\right)}, \quad (31)$$

and ϕ given by (33) shown at the bottom of the next page. Note that B_{β_i} is the residual term in the Fox H-function considered by removing the respective Gamma function from the condition $\mu_{ij} \neq \frac{U_i}{\alpha_{ij}}$ or $z_{ij}^2 \neq U_i$ in (33). From (30), the diversity order is

$$G_{\text{d}} = \sum_{i=1}^{L} \min(\alpha_{i1}\mu_{i1}/2, \ldots, \alpha_{iN}\mu_{iN}/2, z_{i1}^2/2, \ldots, z_{iN}^2/2),$$
$$(32)$$

that depends on the fading and pointing error parameters.

$$f_\Gamma(\gamma) = \frac{\gamma^{-1}}{2} \left[\prod_{i=1}^{L} \prod_{j=1}^{N} \frac{z_{ij}^2}{\alpha_{ij} \Gamma(\mu_{ij}) \Gamma(m_{ij})} \right]$$

$$\times H^{0,0:[2N,N+1]_{i=1:L}}_{0,1:[2N+1,2N]_{i=1:L}} \left[\begin{array}{c} \Xi_1\sqrt{\gamma} \\ \vdots \\ \Xi_L\sqrt{\gamma} \end{array} \middle| \begin{array}{c} - \\ (1, \{1\}_{i=1:L}) \end{array} \middle| \begin{array}{c} [(1,1), \mathcal{A}_{i1}, \ldots, \mathcal{A}_{iN}, \mathcal{B}_{i1}, \ldots, \mathcal{B}_{iN}]_{i=1:L} \\ [\mathcal{C}_{i1}, \ldots, \mathcal{C}_{iN}, \mathcal{D}_{i1}, \ldots, \mathcal{D}_{iN}]_{i=1:L} \end{array} \right] \quad (26)$$

$$F_\Gamma(\gamma) = \frac{1}{2} \left[\prod_{i=1}^{L} \prod_{j=1}^{N} \frac{z_{ij}^2}{\alpha_{ij} \Gamma(\mu_{ij}) \Gamma(m_{ij})} \right]$$

$$\times H^{0,1:[2N,N+1]_{i=1:L}}_{1,2:[2N+1,2N]_{i=1:L}} \left[\begin{array}{c} \Xi_1\sqrt{\gamma} \\ \vdots \\ \Xi_L\sqrt{\gamma} \end{array} \middle| \begin{array}{c} \left(1, \{\frac{1}{2}\}_{i=1:L}\right) \\ (1, \{1\}_{i=1:L}), \left(0, \{\frac{1}{2}\}_{i=1:L}\right) \end{array} \middle| \begin{array}{c} [(1,1), \mathcal{A}_{i1}, \ldots, \mathcal{A}_{iN}, \mathcal{B}_{i1}, \ldots, \mathcal{B}_{iN}]_{i=1:L} \\ [\mathcal{C}_{i1}, \ldots, \mathcal{C}_{iN}, \mathcal{D}_{i1}, \ldots, \mathcal{D}_{iN}]_{i=1:L} \end{array} \right] \quad (27)$$

$$M_\Gamma(s) = \frac{1}{2} \left[\prod_{i=1}^{L} \prod_{j=1}^{N} \frac{z_{ij}^2}{\alpha_{ij} \Gamma(\mu_{ij}) \Gamma(m_{ij})} \right]$$

$$\times H^{0,1:[2N,N+1]_{i=1:L}}_{1,1:[2N+1,2N]_{i=1:L}} \left[\begin{array}{c} \Xi_1 s^{-\frac{1}{2}} \\ \vdots \\ \Xi_L s^{-\frac{1}{2}} \end{array} \middle| \begin{array}{c} \left(1, \{\frac{1}{2}\}_{i=1:L}\right) \\ (1, \{1\}_{i=1:L}) \end{array} \middle| \begin{array}{c} [(1,1), \mathcal{A}_{i1}, \ldots, \mathcal{A}_{iN}, \mathcal{B}_{i1}, \ldots, \mathcal{B}_{iN}]_{i=1:L} \\ [\mathcal{C}_{i1}, \ldots, \mathcal{C}_{iN}, \mathcal{D}_{i1}, \ldots, \mathcal{D}_{iN}]_{i=1:L} \end{array} \right] \quad (28)$$

$$P_{\text{out}} = \frac{1}{2} \left[\prod_{i=1}^{L} \prod_{j=1}^{N} \frac{z_{ij}^2}{\alpha_{ij} \Gamma(\mu_{ij}) \Gamma(m_{ij})} \right]$$

$$\times H^{0,1:[2N,N+1]_{i=1:L}}_{1,2:[2N+1,2N]_{i=1:L}} \left[\begin{array}{c} \Xi_1\sqrt{\gamma_{\text{th}}} \\ \vdots \\ \Xi_L\sqrt{\gamma_{\text{th}}} \end{array} \middle| \begin{array}{c} \left(1, \{\frac{1}{2}\}_{i=1:L}\right) \\ (1, \{1\}_{i=1:L}), \left(0, \{\frac{1}{2}\}_{i=1:L}\right) \end{array} \middle| \begin{array}{c} [(1,1), \mathcal{A}_{i1}, \ldots, \mathcal{A}_{iN}, \mathcal{B}_{i1}, \ldots, \mathcal{B}_{iN}]_{i=1:L} \\ [\mathcal{C}_{i1}, \ldots, \mathcal{C}_{iN}, \mathcal{D}_{i1}, \ldots, \mathcal{D}_{iN}]_{i=1:L} \end{array} \right]$$
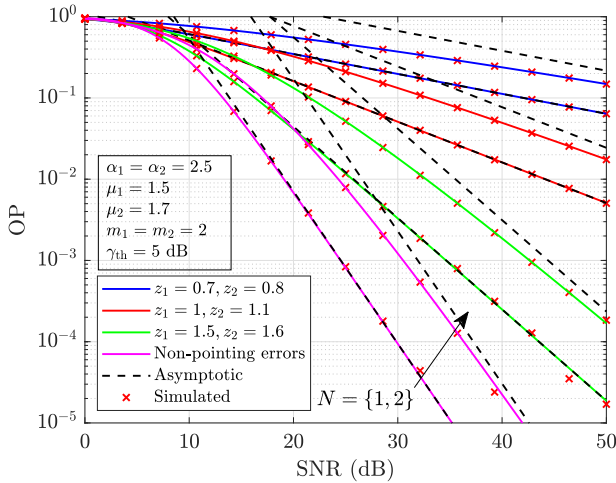$$(29)$$

FIGURE 1. OP curves and their asymptotics as a function of SNR $\bar{\gamma}$, under different values of z_1, z_2, and number of channels N.

IV. NUMERICAL RESULTS

In Fig. 1, the performance of a relaying ($N = 2$) THz wireless communication system is investigated. Theoretical OP curves, from (10), and their asymptotics, from (17), as a function of SNR $\bar{\gamma} = \bar{\gamma}_1 = \bar{\gamma}_2$ are shown, considering strong ($z_1 = 0.7$ and $z_2 = 0.8$), moderate ($z_1 = 1$ and $z_2 = 1.1$), and weak ($z_1 = 1.5$ and $z_2 = 1.6$) pointing error scenarios. Curves without misalignment, i.e. under non-pointing errors, are also presented as benchmarks, obtained when $\{z_1, z_2\} \to \infty$. For comparison purposes, the OP performance of a single ($N = 1$) THz link is also presented. The correctness of the derived expressions is unequivocally confirmed by the excellent correspondence between the theoretical expressions and the simulation curves. Fig. 1 shows that (i) for a fixed SNR, the OP increases as the parameter that characterizes the pointing error (z) decreases, and (ii) the impact of the z on the OP is smaller as N increases. Considering that the channel parameters are equal, the OP of the two-hop relaying THz system is higher than that of the single THz link. Furthermore, the results show that the asymptotic curves coincide with the analytical curves at high SNR values, again corroborating the correctness of the analytical results. As attested by our theoretical findings, the diversity order, which is represented by the slope of asymptotic curves, depended only on the channel non-linearity and the pointing error parameter. For example, when the diversity gain equals $G_d = z_2^2/2 = 1.125$, $z_1 = 1.5$ and $z_2 = 1.6$, the curves for $N = 1$ and $N = 2$ have the same slope at high transmitted power.
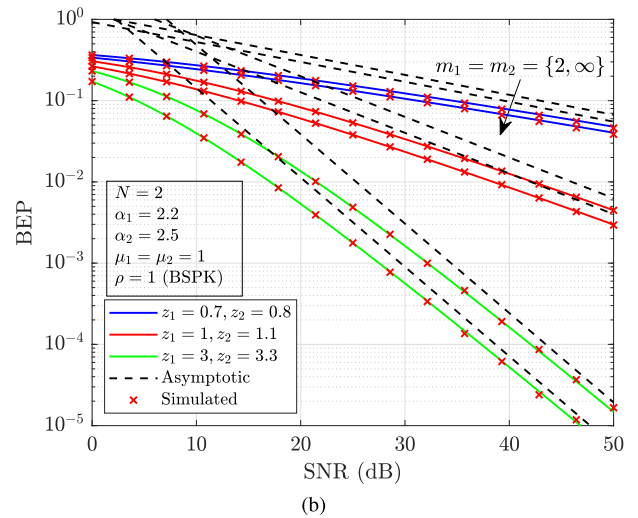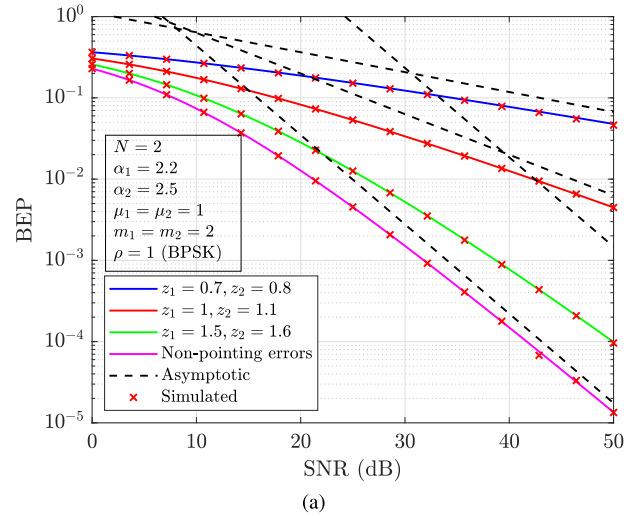

(a)

(b)

FIGURE 2. BEP and asymptotic BEP curves as a function of SNR $\bar{\gamma}$, under different values of (a) z; (b) m and z.

BEP and asymptotic BEP curves as a function of SNR $\bar{\gamma}$ are presented in Fig. 2, under strong, moderate, and weak pointing error conditions with $N = 2$. In all cases, for $\mu = \mu_1 = \mu_2 = 1$, the cascaded shadowed Weibull fading model with pointing errors is obtained as a particular case of the study proposed in this work. To the best of the authors' knowledge, results for the cascaded shadowed Weibull model with the aforementioned effect have not been presented in the literature. The non-pointing errors (obtained when $\{z_1, z_2\} \to \infty$) and no-shadowing (obtained when $m_1 = m_2 = m \to \infty$) cases are included in Fig. 2(a) and (b) as benchmarks, respectively. In

$$\phi = \frac{\prod_{\substack{j=1 \\ \mu_{ij} \neq \frac{U_i}{\alpha_{ij}}}}^{N} \Gamma\left(\mu_{ij} - \frac{U_i}{\alpha_{ij}}\right) \prod_{\substack{j=1 \\ z_{ij}^2 \neq U_i}}^{N} \Gamma\left(\frac{z_{ij}^2 - U_i}{\alpha_{ij}}\right) \prod_{j=1}^{N} \Gamma\left(m_{ij} + \frac{U_i}{\alpha_{ij}}\right)}{\prod_{j=1}^{N} \Gamma\left(\frac{z_{ij}^2}{\alpha_{ij}} + 1 - \frac{U_i}{\alpha_{ij}}\right)} \quad (33)$$
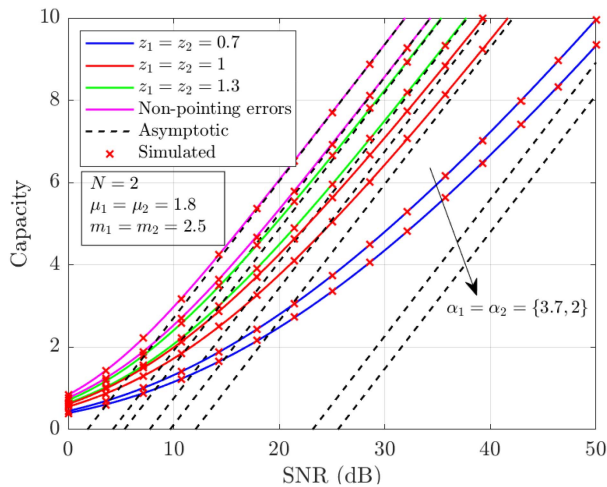
FIGURE 3. Channel capacity and asymptotic channel capacity curves as a function of SNR $\bar{\gamma}$ for different α and pointing error conditions.

Fig. 2(b), the purpose is to provide evidence of the impact of parameter m in the system performance. It can be seen in both figures that the performance degrades as $\{z_1, z_2\}$ decreases. Furthermore, as shown in Fig. 2(b) for lower values of $\{z_1, z_2\}$, almost no impact has the shadowing intensity m in the BEP curves. In addition, the asymptotic curves have the same slope regardless of the value of m.

The performance of amplify-and-forward relaying THz systems in terms of the channel capacity is investigated in Fig. 3, for different values of $\alpha_1 = \alpha_2 = \alpha$ and pointing error conditions. The capacity improves as α and/or $z_1 = z_2$ increases since lower is the effect of the non-linearity and pointing errors in the system. Note that the best capacity curves are for the case in which non-pointing errors are considered. For $\alpha = 2$, the channel capacity corresponding to the cascaded Fisher-Snedecor $\mathcal{F}$ with pointing errors is presented as a benchmark.

AUC and asymptotic AUC curves are presented in Fig. 4, under different number of channels and considering particular cases of our study. It should be mentioned that the AUC metric assumes values between 0.5 and 1 and is used to evaluate the performance of the energy detection schemes. In Fig. 4, AUC curves for the Fisher Snedecor $\mathcal{F}$ and Weibull-$\mathcal{F}$ with pointing errors channels are presented. The mentioned cases are not analyzed in the literature, according to the best authors' knowledge. As the SNR increases, the detection performance gets better. It is noted in Fig. 4 that the energy detector performance depends on the fading parameters. As $\mu_1 = \mu_2 = \mu$ increases, the capability detection is improved. This occurs because of the advantages of the multipath effect. As benchmarks, AUC curves without pointing errors are also presented.

OP and asymptotic OP curves are presented in Fig. 5, under RIS-assisted scenarios considering α-$\mathcal{F}$ fading with pointing errors, for different numbers of the elements L present in the RIS and $\{z_1, z_2\}$ values. In our study, the non-pointing error

(a)

(b)
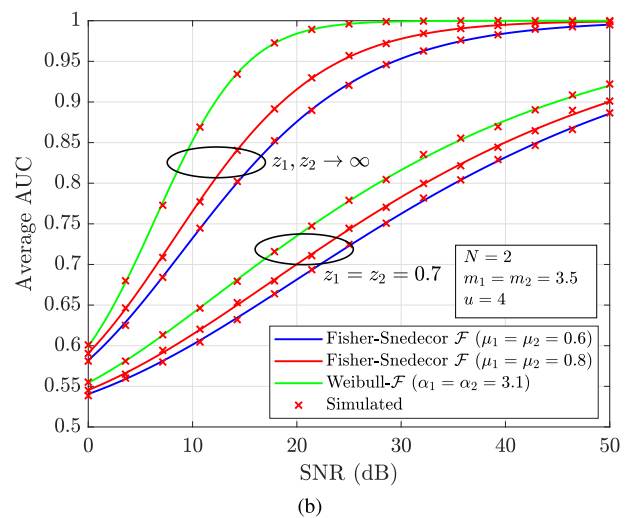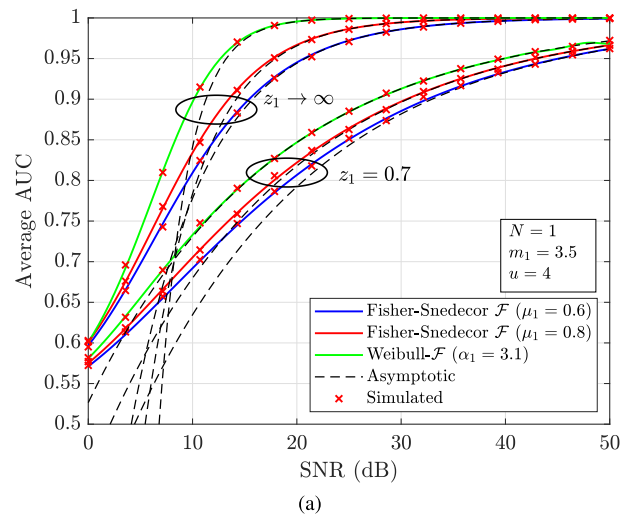
FIGURE 4. AUC and asymptotic AUC curves as a function of SNR $\bar{\gamma}$ for different fading models and number and channels.
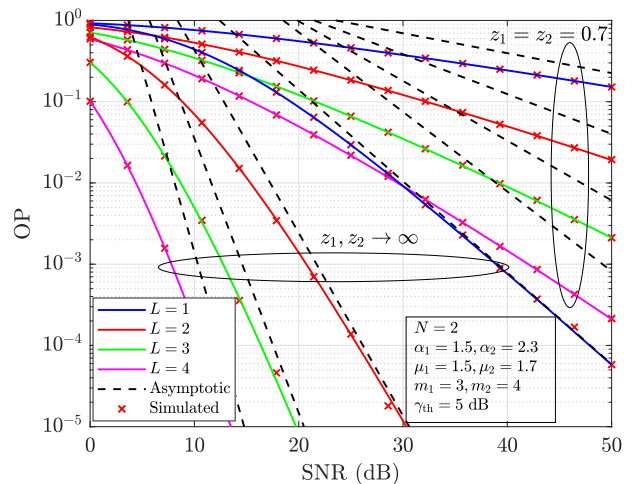
FIGURE 5. OP and asymptotic OP curves as a function of SNR $\bar{\gamma}$, under RIS-assisted scenarios considering α-$\mathcal{F}$ fading with and without pointing error condition.

$$f_H(h) = \frac{1}{h} \left[\prod_{j=1}^{N} \frac{z_j^2}{\alpha_j \Gamma(\mu_j) \Gamma(m_j)} \right] H_{2N,2N}^{2N,N} \left[\prod_{j=1}^{N} \frac{\Psi_j^{1/\alpha_j}}{\hat{r}_j h_{1_j} A_{0_j}} \,\middle|\, \begin{matrix} \mathcal{A}_1, \ldots, \mathcal{A}_N, \mathcal{B}_1, \ldots, \mathcal{B}_N \\ \mathcal{C}_1, \ldots, \mathcal{C}_N, \mathcal{D}_1, \ldots, \mathcal{D}_N \end{matrix} \right] \tag{34}$$

$$f_S(s) = \frac{1}{s} \left[\prod_{i=1}^{L} \prod_{j=1}^{N} \frac{z_{ij}^2}{\alpha_{ij} \Gamma(\mu_{ij}) \Gamma(m_{ij})} \right]$$

$$\times H_{0,1:[2N+1,2N]_{i:L}}^{0,0:[2N,N+1]_{i:L}} \left[\begin{matrix} \Omega_1 s \\ \vdots \\ \Omega_L s \end{matrix} \,\middle|\, \begin{matrix} - \\ (1, \{1\}_{i:1:L}) \end{matrix} \,\middle|\, \begin{matrix} [(1,1), \mathcal{A}_{i1}, \ldots, \mathcal{A}_{iN}, \mathcal{B}_{i1}, \ldots, \mathcal{B}_{iN}]_{i:1:L} \\ [\mathcal{C}_{i1}, \ldots, \mathcal{C}_{iN}, \mathcal{D}_{i1}, \ldots, \mathcal{D}_{iN}]_{i:1:L} \end{matrix} \right] \tag{35}$$

condition is also considered. It should be mentioned that the scenario analyzed in this case corresponds to the sum of the product of two random variables. Note from Fig. 5 that the RIS improves the OP performance. In fact, as L increases, the OP values are lower.

V. CONCLUSION

Statistics have been derived in this paper, such as the PDF, CDF, and MGF of the instantaneous SNR, as well as important metrics, considering cascaded and sum of cascaded α-$\mathcal{F}$ RVs with pointing errors. Curves have been presented for the mentioned metrics, with a strong adherence between the theoretical and simulated points. In addition, the cascaded α-$\mathcal{F}$ distribution with pointing errors has been performed under relaying THz links and RIS-assisted systems.

The overall expressions have been written in terms of a single Fox H-function when dealing with the proposed cascaded of α-$\mathcal{F}$ RVs with pointing errors. However, when dealing with the sum of cascaded, over the application on the channel characterization of RIS systems, the mathematical complexity has led to intricate expressions. So far, if it is possible, we have been unable to find a simpler expression under this comprehensive scenario. Based on some simplifications available elsewhere in the literature, we conjecture that there may be ways to find simpler expressions under not-so-restrictive assumptions. For instance, using discrete values for the number of multipath clusters, i.e., for the corresponding μ parameter, may simplify the expressions. However, this can be a trick task provided that even some already reported particular cases in the literature have been given in terms of the multivariate Fox H-function. But this requires further investigation. This is indeed an interesting opportunity for future work.

APPENDIX A

Let $H = H_1 H_2 \cdots H_N$, where $f_{H_j}(h_j)$, with $j = 1, 2, \ldots, N$, is given by (1). The Mellin transform of $f_{H_j}(h_j)$, denoted by $\mathcal{M}[f_{H_j}(h_j)]$, can be derived by using [30, Eq. (2.9)] and making the variable change $r = h_j^{\alpha_j}$. According to [38, Eq. (3.5)], $\mathcal{M}[f_H(h)] = \mathcal{M}[f_{H_1}(h_1)]\mathcal{M}[f_{H_2}(h_2)] \cdots \mathcal{M}[f_{H_N}(h_N)]$, and the PDF of H can be deduced by using [38, Eq. (3.2)]. After simplifications, (34), shown at the top of this page, is obtained with $\mathcal{A}_j = (1 - m_j, 1/\alpha_j)$, $\mathcal{B}_j = (z_j^2/\alpha_j + 1, 1/\alpha_j)$,

$\mathcal{C}_j = (\mu_j, 1/\alpha_j)$, and $\mathcal{D}_j = (z_j^2/\alpha_j, 1/\alpha_j)$. Making $\Gamma = H^2$, the PDF of the instantaneous SNR (5) can be obtained by using the fact that $f_\Gamma(\gamma) = f_H(\sqrt{\gamma})/(2\sqrt{\gamma})$. Integrating (5), knowing that $\int_0^\gamma x^{n-1}\mathrm{d}x = \gamma^n/n$ and $\Gamma(\gamma + 1) = \gamma\Gamma(\gamma)$, (6) is obtained. The MGF of Γ in (7) is obtained by making the Laplace transform of (5) and proceeding with some simplifications. Hence, the proof is concluded.

APPENDIX B

Let be $S = Z_1 + Z_2 + \cdots + Z_L$, in which $f_{Z_i}(z)$ is given by (34). The MGF of S is given by $M_S(s) = M_{Z_1}(s)M_{Z_2}(s) \cdots M_{Z_L}(s)$, with each $M_{Z_i}(s)$ being obtained by making the Laplace transform of $f_{Z_i}(z)$. Using [30, Eq. (A.13)], the product of the individual MGFs, $M_S(s)$, can be derived in terms of the multivariate Fox H-function. Furthermore, using the Laplace inverse transform of $M_S(s)$ and writing the multivariate Fox H-function in its integral form [30, Eq. A.1], the Laplace inverse transform integral can be internalized. Then, making the variable change $-t = sz$ and solving the inner integral, it is possible to use the fact that $\frac{1}{\Gamma(x)} = \frac{w}{2\pi} \int_C (-t)^{-x} e^{-t} \mathrm{d}t$ to write the envelope PDF $f_S(s)$ in terms of another multivariate Fox H-function. After simplifications, (35), shown at the top of this page, is deduced with $\Omega_i = \prod_{j=1}^{N} \Psi_{ij}^{1/\alpha_{ij}}/(\hat{r}_{ij} h_{1_{ij}} A_{0_{ij}})$ and $\Psi_{ij} = \mu_{ij}/(m_{ij} - 1)$.

The PDF of the instantaneous SNR $\Gamma = S^2$ can be deduced by making $f_\Gamma(\gamma) = f_S(\sqrt{\gamma})/(2\sqrt{\gamma})$, which results in (26). By integrating (26) and by using similar steps presented in Appendix A, the CDF in (27) is obtained. The MGF of Γ shown in (28) is obtained by making the Laplace transform of (26) with some algebraic manipulations. Hence, the proof is concluded.

REFERENCES

[1] O. S. Badarneh, S. Muhaidat, P. C. Sofotasios, S. L. Cotton, K. Rabie, and D. B. da Costa, "The $N*$Fisher-Snedecor F cascaded fading model," in *Proc. IEEE 14th Int. Conf. Wireless Mobile Comput. Netw. Commun.*, 2018, pp. 1–7.

[2] G. K. Karagiannidis, N. C. Sagias, and P. T. Mathiopoulos, "$N*$Nakagami: A novel stochastic model for cascaded fading channels," *IEEE Trans. Commun.*, vol. 55, no. 8, pp. 1453–1458, Aug. 2007.

[3] L. Kong, Y. Ai, S. Chatzinotas, and B. Ottersten, "Effective rate evaluation of RIS-assisted communications using the sums of cascaded α-μ random variates," *IEEE Access*, vol. 9, pp. 5832–5844, 2021.

[4] Y. Chen, Y. Wang, J. Zhang, and M. D. Renzo, "QoS-driven spectrum sharing for reconfigurable intelligent surfaces (RISs) aided vehicular networks," *IEEE Trans. Wireless Commun.*, vol. 20, no. 9, pp. 5969–5985, Sep. 2021.

[5] Y. Chen, Y. Wang, and L. Jiao, "Robust transmission for reconfigurable intelligent surface aided millimeter wave vehicular communications with statistical CSI," *IEEE Trans. Wireless Commun.*, vol. 21, no. 2, pp. 928–944, Feb. 2022.

[6] Y. Chen, Y. Wang, Z. Wang, and P. Zhang, "Robust beamforming for active reconfigurable intelligent omni-surface in vehicular communications," *IEEE J. Sel. Areas Commun.*, vol. 40, no. 10, pp. 3086–3103, Oct. 2022.

[7] L. Kong, G. Kaddoum, and D. B. da Costa, "Cascaded α-μ fading channels: Reliability and security analysis," *IEEE Access*, vol. 6, pp. 41978–41992, 2018.

[8] Y. Alghorani, G. Kaddoum, S. Muhaidat, S. Pierre, and N. Al-Dhahir, "On the performance of multihop-intervehicular communications systems over n*Rayleigh fading channels," *IEEE Wireless Commun. Lett.*, vol. 5, no. 2, pp. 116–119, Apr. 2016.

[9] T. Bao, H. Wang, H. -C. Yang, W. -J. Wang, and M. O. Hasna, "Performance analysis of RIS-aided communication systems over the sum of cascaded Rician fading with imperfect CSI," in *Proc. IEEE Wireless Commun. Netw. Conf.*, 2022, pp. 399–404.

[10] A. A. Farid and S. Hranilovic, "Outage capacity optimization for freespace optical links with pointing errors," *J. Lightw. Technol.*, vol. 25, no. 7, pp. 1702–1710, Jul. 2007.

[11] A.-A. A. Boulogeorgos, E. N. Papasotiriou, and A. Alexiou, "Analytical performance assessment of THz wireless systems," *IEEE Access*, vol. 7, pp. 11436–11453, 2019.

[12] A. -A. A. Boulogeorgos, N. D. Chatzidiamantis, H. G. Sandalidis, A. Alexiou, and M. D. Renzo, "Cascaded composite turbulence and misalignment: Statistical characterization and applications to reconfigurable intelligent surface-empowered wireless systems," *IEEE Trans. Veh. Technol.*, vol. 71, no. 4, pp. 3821–3836, Apr. 2022.

[13] V. K. Chapala and S. M. Zafaruddin, "Exact analysis of RIS-aided THz wireless systems over α-μ fading with pointing errors," *IEEE Commun. Lett.*, vol. 25, no. 11, pp. 3508–3512, Nov. 2021.

[14] O. R. Durgada, V. K. Chapala, and S. M. Zafaruddin, "RIS-THz wireless communication with random phase noise and misaligned transceiver," *ArXiv*, pp. 1–6, Nov. 2022.

[15] O. S. Badarneh, R. Mesleh, and Y. M. Khattabi, "Reconfigurable intelligent surfaces-assisted terahertz communications," *J. Franklin Inst.*, vol. 359, no. 18, pp. 11256–11272, Dec. 2022.

[16] S. H. Alvi et al., "Performance analysis of IRS-assisted THz communication systems over α-μ fading channels with pointing errors," *Sensors*, vol. 23, no. 16, pp. 1–20, Aug. 2023.

[17] E. N. Papasotiriou, S. Droulias, and A. Alexiou, "Analytical characterization of RIS-aided terahertz links in the presence of beam misalignment," *IEEE J. Sel. Topics Signal Process.*, vol. 17, no. 4, pp. 850–860, Jul. 2023.

[18] V. K. Chapala and S. M. Zafaruddin, "Multiple RIS-assisted mixed FSO-RF transmission over generalized fading channels," *IEEE Syst. J.*, vol. 17, no. 3, pp. 3515–3526, Sep. 2023.

[19] S. Sai and L. Yang, "Performance analysis of dual-hop THz transmission systems over α-μ fading channels with pointing errors," *IEEE Internet Things J.*, vol. 9, no. 14, pp. 11772–11783, Jul. 2022.

[20] P. Bhardwaj and S. M. Zafaruddin, "On the performance of multi-hop THz wireless system over mixed channel fading with shadowing and antenna misalignment," *IEEE Trans. Commun.*, vol. 70, no. 11, pp. 7748–7763, Nov. 2022.

[21] L. Cang et al., "Terahertz MIMO communication performance analysis in exponentiated Weibull turbulence with pointing errors," *Appl. Opt.*, vol. 60, no. 24, pp. 7314–7325, Aug. 2021.

[22] Z. Ding and H. V. Poor, "Design of THz-NOMA in the presence of beam misalignment," *IEEE Commun. Lett.*, vol. 26, no. 7, pp. 1678–1682, Jul. 2022.

[23] O. S. Badarneh, "The α-$\mathcal{F}$ composite fading distribution: Statistical characterization and applications," *IEEE Trans. Veh. Technol.*, vol. 69, no. 8, pp. 8097–8106, Aug. 2020.

[24] R. Bhatnagar and P. Garg, "Hybrid underwater wireless system for shallow sea monitoring: An outage analysis," in *Proc. IEEE Int. Conf. Electron. Comput. Commun. Technol.*, 2022, pp. 1–5.

[25] Q. Sun, Z. Zhang, Y. Zhang, M. López-Benítez, and J. Zhang, "Performance analysis of dual-hop wireless systems over mixed FSO/RF fading channel," *IEEE Access*, vol. 9, pp. 85529–85542, 2021.

[26] R. Bhatnagar and P. Garg, "Performance analysis of hybrid underwater wireless system for shallow sea monitoring," *Photon. Netw. Commun.*, vol. 46, pp. 78–89, 2023.

[27] R. Bhatnagar and P. Garg, "Parametric evaluation of decode and forward relay based mixed wireless transmission system over α-$\mathcal{F}$ fading channels," in *Proc. IEEE Int. Conf. Sustain. Emerg. Innov. Eng. Technol.*, 2023, pp. 15–18.

[28] M. T. Dabiri, M. Hasna, N. Zorba, T. Khattab, and K. A. Qaraqe, "A general model for pointing error of high frequency directional antennas," *IEEE Open J. Commun. Soc.*, vol. 3, pp. 1978–1990, 2022.

[29] M. T. Dabiri and M. Hasna, "Pointing error modeling of mmWave to THz high-directional antenna arrays," *IEEE Wireless Commun. Lett.*, vol. 11, no. 11, pp. 2435–2439, Nov. 2022.

[30] A. M. Mathai, R. K. Saxena, and H. J. Haubold. *The H-Function: Theory and Applications*. New York, NY, USA: Springer, 2009.

[31] P. H. D. Almeida, L. R. Andrade, H. S. Silva, U. S. Dias, O. S. Badarneh, and R. A. A. de Souza, "The α-$\mathcal{F}$ composite distribution with pointing errors: Theory and applications to RIS," *J. Franklin Inst.*, vol. 361, no. 10, pp. 1–13, Jul. 2024.

[32] Wolfram Research, Inc., 2020. Dec. 16, 2022. [Online]. Available: http://functions.wolfram.com/id

[33] A. A. Kilbas and M. Saigo, *H-Transforms: Theory and Applications*. Boca Raton, FL, USA: CRC Press, 2004.

[34] S. K. Yoo, P. C. Sofotasios, S. L. Cotton, S. Muhaidat, O. S. Badarneh, and G. K. Karagiannidis, "Entropy and energy detection-based spectrum sensing over $\mathcal{F}$-composite fading channels," *IEEE Trans. Commun.*, vol. 67, no. 7, pp. 4641–4653, Jul. 2019.

[35] I. S. Gradshteyn and I. M. Ryzhik, *Table of Integrals, Series and Products*. San Francisco, CA, USA: Academic Express, 2007.

[36] Y. A. Rahama, M. H. Ismail, and M. S. Hassan, "On the sum of independent Fox's H-function variates with applications," *IEEE Trans. Veh. Technol.*, vol. 67, no. 8, pp. 6752–6760, Aug. 2018.

[37] F. Yilmaz and M.-S. Alouini, "Novel asymptotic results on the high-order statistics of the channel capacity over generalized fading channels," in *Proc. IEEE 13th Int. Workshop Signal Process. Adv. Wireless Commun.* 2012, pp. 389–393.

[38] M. D. Springer and W. E. Thompson, "The distribution of products of independent random variables," *SIAM J. Appl. Math.*, vol. 14, no. 3, pp. 511–526, May 1966.

PEDRO H. D. ALMEIDA (Graduate Student Member, IEEE) received the B.Sc. degree in communication network engineering in 2023 from the University of Brasília, Brasília, Brazil, where he is currently working toward the M.Sc. degree. His main research interests include digital signal processing and mobile networks.

HUGERLES S. SILVA (Senior Member, IEEE) received the B.Sc., M.Sc., and Ph.D. degrees in electrical engineering from the Federal University of Campina Grande, Campina Grande, Brazil, in 2014, 2016, and 2019, respectively. In 2021, he joined the University of Brasília, Brasília, Brazil, where he is currently a Professor. He is also a Researcher with the Telecommunications Institute in Portugal. His main research interests include wireless communication, digital signal processing, and wireless channel modeling.

UGO S. DIAS (Senior Member, IEEE) was born in Belém, Brazil, in 1981. He received the B.Sc. degree in electrical engineering from The Federal University of Pará, Belém, Brazil, in 2004, and the M.Sc. and Ph.D. degrees in electrical engineering from the State University of Campinas, Campinas, Brazil, in 2006 and 2010, respectively. Since 2010, he has been a Professor with the University of Brasilia, Brasília, Brazil. He is currently a Faculty Member with the Department of Electrical Engineering. Prof. Dias has been involved on the Organizing Committee of several conferences. He acts as a Scientific Consultant for the National Council of Scientific and Technological Development (CNPq), Brasília, and where he is also a Productivity Research Fellow. He is currently the President of the Brazilian Telecommunications Society, Chair of the IEEE ComSoc CN Brazil Chapter, and an Advisor of the IEEE ComSoc UnB Student Branch Chapter. He is also a Senior Member of SBrT, and a Member of IEEE Communications Society and Brazilian Communications Committee.

RAUSLEY A. A. DE SOUZA (Senior Member, IEEE) received the B.S.E.E. and M.Sc. degrees from the National Institute of Telecommunications (INATEL), Santa Rita do Sapucaí, Brazil, in 1994 and 2002, respectively, and the Ph.D. degree from the State University of Campinas, Campinas, Brazil. Prior to joining the academy, he worked in the industry. In 2002, he joined the INATEL where he is currently a Full Professor. His research focuses on wireless communications.

IGUATEMI E. FONSECA received the Electronics Engineering degree from the Federal University of Campina Grande (UFCG), Campina Grande, Brazil, in 1999, and the M.Sc. and Ph.D. degrees from the State University of Campinas (Unicamp), Campinas, Brazil, in 2001 and 2005, respectively. He is currently an Associate Professor with the Informatics Center of the Federal University of Paraíba, Belém, Brazil. His research interests include communications networks, working on topics as identification of traffic in computer networks, techniques for identification and mitigation of DDoS attacks, algorithms and protocols in industrial wireless sensor networks, and WDM and elastic optical networks with QoS requirements.

YONGHUI LI (Fellow, IEEE) received the Ph.D. degree from the Beijing University of Aeronautics and Astronautics, Beijing, China, in 2002. Since 2003, he has been with the Centre of Excellence in Telecommunications, The University of Sydney, Sydney, NSW, Australia. He is currently a Professor and the Director of Wireless Engineering Laboratory, School of Electrical and Information Engineering, University of Sydney. His research interests include the area of wireless communications, with a particular focus on MIMO, millimeter wave communications, machine to machine communications, coding techniques, and cooperative communications. He holds a number of patents granted and pending in these fields. He was an Editor of IEEE Transactions on Communications and IEEE Transactions on Vehicular Technology. He was a Guest Editor for several IEEE journals, such as IEEE Journal on Selected Areas in Communications, *IEEE Communications Magazine*, IEEE Internet of Things Journal, and IEEE Access. He was the recipient of the Best Paper Awards from IEEE International Conference on Communications (ICC) 2014, IEEE PIRMC 2017, and IEEE Wireless Days Conferences (WD) 2014. He was also the recipient of the Australian Queen Elizabeth II Fellowship in 2008 and the Australian Future Fellowship in 2012.